Luminescence and resonant Raman scattering of color centers in irradiated crystalline L-alanine

E. Winkler, P. Etchegoin, A. Fainstein, and C. Fainstein
Centro Atómico Bariloche & Instituto Balseiro, Comisión Nacional de Energía Atómica & Universidad Nacional de Cuyo, 8400-San Carlos de Bariloche, Río Negro, Argentina
(Received 17 December 1997)

The color centers in electron irradiated L-alanine crystals are studied by means of resonant Raman scattering and photoluminescence. We find a selective resonant enhancement of some of the Raman-active vibrations. The Raman resonant modes are either localized at the methyl group or belong to lattice modes comprising displacements of the ammonium group in the damaged amino acid molecules. The luminescence intensity wanes with increasing temperature above an onset of ~150 K, indicating a strong interaction of the photoexcited electrons in the defects with the lattice modes. These results are compared with the electron-paramagnetic-resonance absorption brought forth by these defects. A simple model calculation that explains the experimental results qualitatively is presented. It is shown that optical spectroscopy provides a valuable technique to study color centers in organic crystals on account of the spatial information of the wave function that can be obtained by resonant Raman scattering. [S0163-1829(98)03221-4]

I. MOTIVATION

Amino acid crystals constitute important model systems for the physical properties of more complex macromolecules such as proteins, metalloproteins, and nucleic acids.[1] Besides this fundamental interest, crystalline alanine $[CH_3CH(NH_2)COOH]$ has proven to be a good candidate for applications in irradiation dosimetry. The reason is twofold: its linearity in a large range of radiation doses, and its superior time stability to record such events. Irradiation induced defects show no substantial decay over periods of 20 years at room temperature.[2] The irradiation induced defects can be quantified and have been mainly studied by electron paramagnetic resonance (EPR),[3–5] and by related techniques such as electron-nuclear double resonance (ENDOR) (Ref. 6) and longitudinally modulated ENDOR (LOMENDOR).[7] In fact, the hyperfine structure of irradiation produced free radicals in alanine crystals provides important information on the symmetry and dynamics of the defects.

The EPR spectra of irradiated single crystals of alanine, for the magnetic field along the *c* axis, is characterized by five lines at room temperature that split in a more complex structure below ~120 K.[3–5] The interpretation of these spectra as produced by a spin-$\frac{1}{2}$ coupled through the hyperfine interaction to four protons, has enabled an assignment of the defect as a dangling electron produced by the breaking of the bond linking the ammonium group (NH_2) with the rest of the molecule. The unpaired electron is mainly localized at the CH and methyl (CH_3) groups. The temperature dependence of the spectra has been associated with the dynamics of the methyl group; its accelerating rotation with increasing temperature produces a *hyperfine interaction averaging*, similar in many respects to the phenomenon of motional narrowing. Besides the induced magnetic resonance absorption, the electron irradiation damage in alanine generates color centers producing a yellowish appearance to the naked eye in the otherwise transparent samples. However, to the best of our knowledge, no study of the luminescence and Raman spectra of vibrational modes linked to the damaged molecules has been reported up to the present, in spite of the rich information that these techniques can provide regarding the electronic structure and dynamics of the defects.

We have carried out a comprehensive study of electron irradiation induced defects in crystalline L-alanine by optical techniques. The Raman and infrared spectra of nonirradiated L-alanine crystals have been extensively studied in the past.[8–10] While the low-frequency portion of the spectra originates in lattice modes propagating through the whole crystal, higher energy modes have been clearly identified as due to intramolecular vibrations localized in different parts of the molecule. This specificity of the vibrational spectra is exploited in our investigations as a localized probe of the defect electron wave function and its spatial extension. This is accomplished by studying the selective resonant enhancement of spectral features. In fact, Raman scattering by vibrations in insulators is mediated by excitonic transitions and its efficiency dependence with laser energy can hence be used to gain information on the electronic structure and electron-phonon interaction.[11] We found that a broad inhomogeneously broadened luminescence centered at about 2.25 eV characterizes the emission spectra of irradiated samples and that only particular modes, basically comprising vibrations of the methyl *but also the ammonium* group, resonate when the laser energy is varied around this energy. These results imply that the defect wave function extends not only to the methyl and CH groups, as inferred from the magnetic-resonance experiments, but also significantly to the separated NH_2 group. Further support for this picture is found in the temperature dependence of the luminescence, which shows an intensity decrease above an onset of ~150 K and which can be linked to the interaction of the photoexcited electron, localized in the defect, with the same ammonium related phonon modes observed to display a resonant Raman behavior. These conclusions are further supported by a calculation of the electronic structure of a damaged L-alanine molecule.

The paper is organized as follows. Section II describes the magnetic resonance and optical spectroscopy experimental setup as well as the samples used in this investigation. We

proceed to present our magnetic-resonance results in Sec. III, as a brief overview of the current knowledge on irradiation induced defects in L-alanine. The Raman spectra and their assignment, the resonant Raman-scattering results, and the luminescence data as a function of temperature follow in Sec. IV. A brief calculation of the electronic structure of a defect in L-alanine is presented in Sec. V and, finally, a few conclusions are presented in Sec. VI.

II. EXPERIMENTAL SETUP AND SAMPLES

EPR absorption experiments as a function of temperature between 77 K and 300 K were carried out at X-band (9 GHz) on a Bruker ESP300 spectrometer. The luminescence and Raman spectra, on the other hand, were recorded on a Jobin-Yvon T64000 triple spectrometer working in substractive mode, also in the 77–300 K range. CCD multichannel and phototube (single-channel) detection were used according to the need for the optical experiments. Typical resolutions were around 1 cm^{-1} for the Raman spectra, and 2 nm for the luminescence scans in single-channel detection. The luminescence spectra were excited with the 454.5 nm line of an Ar^+ laser. For the resonant Raman spectra the nine Ar^+ laser lines, ranging from 514.5 to 454.5 nm, and a single mode polarized He-Ne laser (632.8 nm, 5 mW) were employed as excitation. Input laser powers up to 200 mW for the Ar^+ laser and spots of ~ 100 μm in diameter were used. The Raman-scattering experiments were performed in a backscattering configuration, with excitation and collection along the a crystal axis and parallel polarizations along b [$a(b,b)\bar{a}$ in the Porto's notation[11]].

L-alanine single crystals were grown by slow evaporation of an aqueous solution at room temperature. The obtained crystals show well-defined {120} faces, the intersection of which defines a c axis that enables easy positioning for the magnetic resonance and polarized optical experiments. The irradiation of the samples was accomplished by a 2.5 MeV electron beam at the LINAC facility of the Centro Atómico Bariloche, typically from a few seconds to some minutes. Several samples with up to 0.2% of irradiation damaged molecules were studied. Dose uniformity through the crystal volume was assured by rotation of the sample normal to the electron-beam direction during the irradiation periods.

III. ELECTRON PARAMAGNETIC RESONANCE

In this section we will present our EPR absorption data on irradiated L-alanine crystals. However, since a comprehensive and detailed account of these results can be found in the literature,[3–5] we will only briefly dwell on them to introduce the established knowledge concerning the free radical left by irradiation damage. We shall also use these results to ascertain the quality and characteristics of the samples used in our investigation.

The alanine molecule [$CH_3CH(NH_2)COOH$], shown in Fig. 1, can be divided for discussion purposes in a methyl (CH_3) and an ammonium (NH_2) group, linked to a COOH radical by a CH bond. The crystal structure is orthorhombic with four molecules per unit cell, and the link between molecules is established through hydrogen bonding between the oxygens of the COOH radical and the hydrogens of the ammonium group of the neighbor molecule.[12] The COOH radical of L-alanine contributes to the bonding between molecules in the crystal, but has been shown from EPR experiments[3–5] to have no detectable coupling with the irradiation induced electron. The stable free radical produced by irradiation is apparently due to the breaking of the C-NH_2 bond leading to an unpaired electron spatially extending through the CH_3 and CH groups. In fact, the EPR spectrum at high temperatures [T=298 K, shown in Fig. 2(a)], obtained with the magnetic field along the c axis, is composed of five lines that can be well accounted for by a dangling bond model of an unpaired electron coupled through the hyperfine interaction with four equivalent protons.[4] The four protons are assumed to be the three hydrogen atoms in the CH_3 group, made equivalent by the temperature induced methyl group rotation about its axis, plus the hydrogen atom in CH. This conclusion is also supported by the splitting of these lines at lower temperatures [below 120 K, see Fig. 2(b)], which indicates a slowing down of this movement and a consequent differentiation of the hyperfine interaction with each of the hydrogen atoms. The fit of the spectra in Fig. 2 was obtained with a model that includes the hyperfine interaction with the four protons, allowing for the reorientation of the methyl group with a temperature-dependent characteristic time τ (see Ref. 5 for details). There is an overall good agreement. Note however that weaker interactions with, for example, the protons in the ammonium group, could generate some of the unaccounted smaller spectral features, or could also be masked in the relatively large observed linewidths. As we shall comment in Sec. V, these linewidths are also consistent with the existence of a distribution of hyperfine couplings due to inhomogeneously broadened defect electronic states. The integrated intensity of the room-temperature EPR signals in irradiated L-alanine crystals is used as an extremely precise and stable dosimeter,[2] and has been used here to determine the radiation dose of the studied samples.

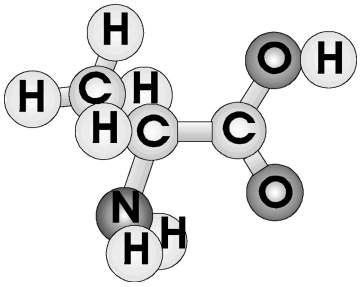

FIG. 1. Molecule of L-alanine. The molecule is basically composed of a CH_3 methyl group, an ammonium (NH_2) group linked to CH, and a COOH radical.

In the next section we present our Raman-scattering and luminescence data that provide a more complete description of the electronic defects in irradiated L-alanine samples through their interaction with molecular and lattice vibrations.

IV. RAMAN SCATTERING AND LUMINESCENCE

The polarized Raman spectrum of L-alanine single crystals has been the subject of a painstaking study in the past,[8]

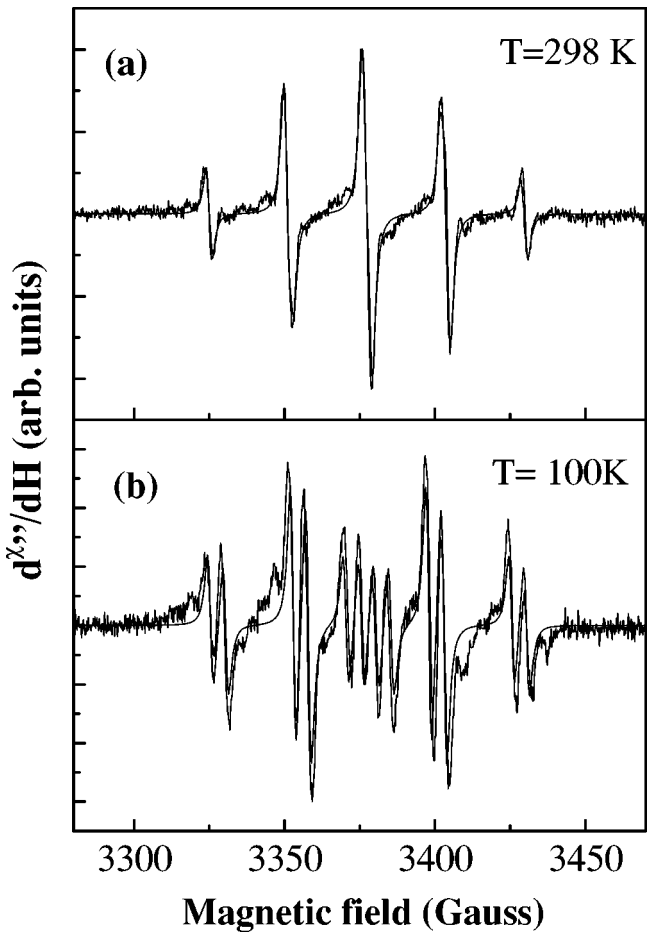

FIG. 2. EPR spectra of an L-alanine irradiated crystal measured at 298 K (a) and 100 K (b). Note the splitting of lines at lower temperatures due to the slowing down of methyl group rotations. The curves are fits with a model that takes into account the hyperfine interaction with the four protons in the CH_3 and CH groups, and allows for the reorientation of the methyl group (see text for details).

in the light of normal mode analysis complementary to infrared transmission spectroscopy.[9,10] For the present aim, we shall not dwell on the full characterization of the modes in view of the fact that we direct our attention solely to those modes that show some resonant behavior with the electronic defects. For the full details of mode labeling, the reader is referred to the exhaustive previous works on the subject.[8–10] In Fig. 3 we show the polarized Raman spectrum of a nonirradiated single crystal of L-alanine at room temperature for the $a(b,b)\bar{a}$ scattering configuration. We shall make a few general comments on the overall characteristics of the spectrum to help in addressing the issues of our interest subsequently. The Raman spectrum of crystalline L-alanine displays modes up to $\sim 3200\ \mathrm{cm}^{-1}$. For the isolated molecule in the form of zwitterion, the lowest vibration is around $\sim 25\ \mathrm{cm}^{-1}$ while the highest is $\sim 3400\ \mathrm{cm}^{-1}$.[13] In the crystal, the presence of four molecules in each unit cell brings forth additional modes called *lattice modes*[8–10] that have their origin in the intermolecular interactions. We shall be concentrating our attention to two types of modes with different origins, to wit: (i) a collection of modes around 2900 cm^{-1} identified as intramolecular stretching of the hydrogens and (ii) a series of low-frequency modes between $\sim 100-120\ \mathrm{cm}^{-1}$ that have their origin in intermolecular interactions through the hydrogen bonds linking different molecules of the unit cell. These latter modes are, therefore, lattice modes[8–10] and have been previously investigated in the framework of hydrogen bonding studies[14] and dynamic localization of phonons.[15] The stretching modes of the hydrogens linked to the nitrogen atom (ammonium group) do not belong to the modes around $\sim 2900\ \mathrm{cm}^{-1}$ because they are modified by the hydrogen bonding to the neighboring oxygens. We can, therefore, consider the modes around 2900 cm^{-1} as completely arising from the methyl group. The lattice modes will be, accordingly, mainly related to the ammonium group. Henceforth, we shall understand *lattice modes* or *stretching modes intensities* as the *integrated* intensities of these vibrations. The spectrum in Fig. 3 has been taken with the 514.5 nm line of the Ar^+ laser, where the nonirradiated crystal is translucent; the spectrum is, accordingly, backgroundless.

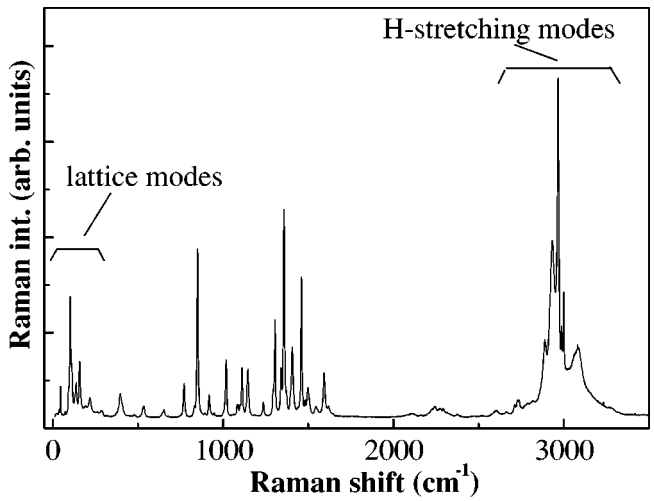

FIG. 3. Raman spectrum in the $a(b,b)\bar{a}$ configuration of a nonirradiated L-alanine single crystal at room temperature. The modes around ~ 2900 and $\sim 100\ \mathrm{cm}^{-1}$ have their origin in intramolecular stretching of the hydrogens in the methyl group and intermolecular hydrogen-bond lattice vibrations in the ammonium group, respectively. These modes show a resonant behavior upon irradiation and are, accordingly, subject to special attention in this study.

Upon irradiation with an electron beam, the sample turns yellowish due to the presence of electronic defects in the gap (color centers) and displays a broad featureless luminescence in the visible. In Fig. 4 we show a sample with 0.1% of damaged molecules, being excited with the different lines of the Ar^+ laser and, additionally, the 632.8 nm line of a low power polarized He-Ne laser. The scattering configuration is the same as in Fig. 3. The salient characteristics of the spectra are summarized as follows: (i) for all lines of the Ar^+ laser the spectra consist of a broad featureless background luminescence and the Raman modes on top. (ii) The shape of the luminescence changes gradually on going from the 514.5 nm to the 454.5 nm excitation lines. This effect comes about because the laser is within the luminescence at 514.5 nm and fully above it at 454.5 nm. (iii) The intensity of the stretching modes can be seen to change with a naked eye, increasing slightly from 514.5 to 472.5 nm excitation, and then remain-

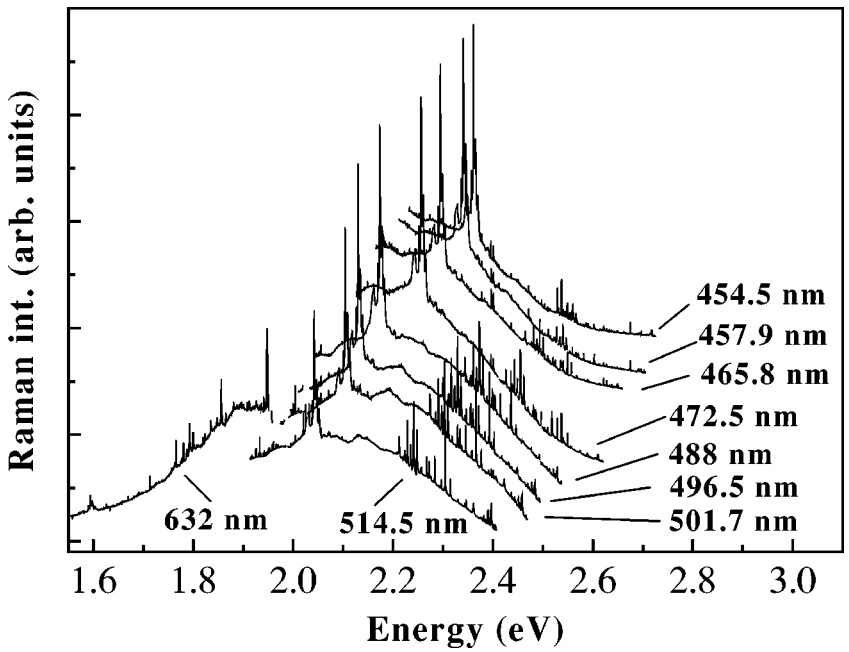

FIG. 4. Raw Raman spectra of an electron-beam irradiated single crystal of L-alanine (0.1% of damaged molecules) at 77 K in the $a(b,b)\bar{a}$ scattering geometry. The different curves belong to distinct excitation lines of the Ar^+ laser ranging from 514.5 to 454.5 nm, and 200 mW for all lines. The curves have been vertically displaced for display purposes. Note the presence of a broad featureless luminescence background below the Raman signals. Note also the change in the intensity of the stretching modes that appear at $\sim$ 2 eV for the 514.5 nm and at $\sim$ 2.4 eV for the 454.5 nm lines, respectively. The spectrum taken with a He-Ne laser is also shown on the left side. Note that the stretching modes are near $\sim$1.6 eV in this case and their intensity has dropped considerably. The luminescence extends from $\sim$1.7 to $\sim$2.7 eV. See text for further details.

ing approximately constant. (iv) The spectrum with the He-Ne laser (632.8 nm) shows the complementary low-energy tail of the luminescence. Note that the stretching modes for this line are weak and approximately located at $\sim$1.6 eV. (v) The lattice modes show the converse behavior of the stretching ones for the Ar^+-laser lines. With the 514.5 nm excitation line the modes are seen as a small peak located approximately at 2.4 eV. Their intensity decreases gradually until they are barely seen for $\hbar\omega_L = 454.5$ nm. Conversely, the lattice modes for the He-Ne laser are situated on top the luminescence at $\sim$1.95 eV and show a considerable enhancement.

The raw data displayed in Fig. 4 give a general outlook and points towards the existence of some interaction between the broad luminescence and both the stretching and lattice modes. Nevertheless, the quantitative analysis of the intensity variations of the peaks has to be corrected by the spectral dependence of the CCD detector. After doing so, it can be shown that stretching and lattice modes do display an enhancement when they are on top of the underlying luminescence, as we shall show later. Perhaps the most direct proof that this happens, and that it is indeed different from the behavior of a nonirradiated crystal, is to compare the Raman signals of two crystals, with and without irradiation, for a fixed laser excitation line. This is done in Fig. 5, where we compare the two spectra for two laser lines. In Fig. 5(a), the laser and the lattice mode's energy are above the luminescence of the irradiated sample while the stretching modes lay within. In Fig. 5(b), on the other hand, the laser (He-Ne, 632.8 nm) and the lattice modes are on top of the low-energy tail of the luminescence while the stretching modes lay below. Though a direct comparison of Raman intensities for two samples with different surface quality and absorption cannot be done, if we arbitrarily set equal the intensity of the *lattice modes* in Fig. 5(a) (inset), the stretching modes integrated intensity is slightly larger (about $\sim$30%) in the irradiated crystal. Contrary to this, when the intensity of the *stretching modes* is set equal in Fig. 5(b), it is the lattice modes on the low-energy tail of the luminescence that show a noteworthy enhancement in the irradiated sample.

The fact that the luminescence is broad and covers most of the visible range thwarts the possibility of observing the full resonant profile of the modes. As can be seen in Fig. 4, the highest laser energy available for excitation (454.5 nm) is not enough to place the stretching modes above the luminescence background. At the same time, the lowest energy line of the Ar^+ laser (514.5 nm) cannot push the stretching modes below the low-energy tail of the luminescence. The lattice modes for the Ar^+-laser lines explore the upper part of the luminescence only. There is, in addition, an abrupt change to the other end for the He-Ne laser, where the stretching modes lay below and the lattice ones on top of the luminescence. We can, however, reconstruct part of the resonance profile if we use the combined data for the two modes with the intensities appropriately normalized. This is shown in Fig. 6(a) where we show the normalized intensities for the stretching and lattice modes for all nine lines of the Ar^+ laser. The normalization with respect to the spectrometer response has been done by dividing the integrated peak intensities at each laser wavelength with the corresponding one measured in a nonirradiated sample. The data points for the stretching modes span the energy range $\sim$ 2.05–2.35 eV, while the lattice modes cover the range $\sim$ 2.4–2.7 eV. If we liken the curve around 2.35 eV we can obtain a fairly good

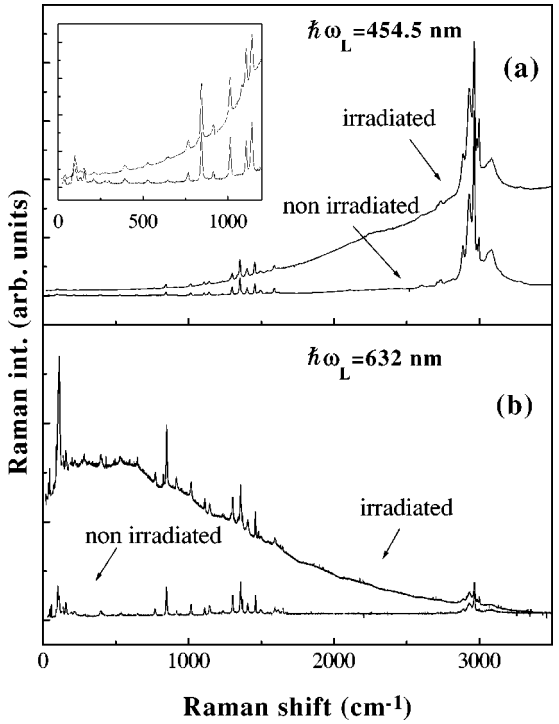

FIG. 5. Comparison between the Raman spectra of two L-alanine crystals with and without irradiation for two different laser lines. In (a), the excitation is done with the 454.5 nm line of the Ar^+ laser. The inset is a blowup of the low-energy region. The laser and the lattice modes are above the maximum of the luminescence, and the intensity of the latter has been set arbitrarily equal for both samples. The stretching modes are enhanced ($\sim$30% in the integrated intensity) for the irradiated sample in this case. In (b), the situation is reversed for the He-Ne laser. The lattice modes on the low energy tail of the luminescence are enhanced for the irradiated sample when the stretching modes intensity is set equal.

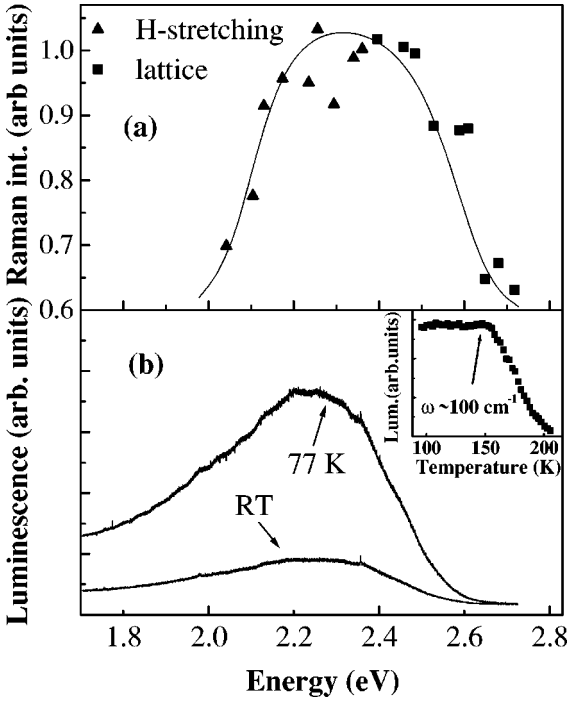

FIG. 6. (a) Normalized (by the incident power and detector response) intensity of the stretching and lattice modes for all nine lines of the Ar^+ laser. The two curves are conveniently matched around 2.3 eV to give a continuous resonance profile. Note that the resonance enhancement is roughly $\sim$50%. The curve is a guide to the eye. In (b) we show the luminescence of a heavily irradiated sample at 77 K and room temperature. Notice that the maximum of the luminescence remains unaltered around $\sim$2.25 eV, implying the absence of thermalization among the electrons producing the luminescence. The inset shows the temperature dependence of the luminescence maximum. Note the crossover around 150 K, which implies a relaxation of the electronic states in the defects through phonons of $\omega \sim 100\ \mathrm{cm}^{-1}$. These modes are the lattice modes that exhibit, at the same time, a resonant behavior in Fig. 5(b). See text for further details.

idea of what the full resonant profile should look like, with the proviso in mind that the coupling of the modes to the electrons that produce the luminescence may be different. Note that only single resonant Raman processes[11] are possible here: a double resonance, that is, an incoming resonance of the laser and a subsequent outgoing resonance of the scattered photon would imply the participation of two electronic states that, in fact, correspond to *different* molecules. The modes at 2900 cm^{-1} are enhanced mainly through an outgoing resonance, while for the lattice modes both incoming and outgoing *single* resonances contribute (the laser and phonon peaks are rather close in the scale of energies covered by the defect states and thus we cannot distinguish both processes). The other prominent feature to be mentioned is that the data in Fig. 6(a) implies a rather weak resonant enhancement that is coarsely a factor of 50%. This weak enhancement has a physical origin that we shall comment upon later.

Finally, we concentrate on the characteristics of the luminescence for the irradiated samples. First, the fact that the luminescence is broad points in the direction of inhomogeneous broadening as the main cause for its width. This broadening has its origin in the distribution of different defects created by the electron-beam irradiation. Moreover, the temperature dependence of this broad emission shows that there is no noticeable change in the position of the maximum, which always stays at $\sim$2.25 eV. This is shown in Fig. 6(b) where the luminescence under the 454.5 nm excitation line is shown for a heavily irradiated sample with 0.2% of damaged molecules. Note that, to avoid the problem of matching several CCD-camera scans, these spectra were acquired using a phototube detector with a relatively large wavelength step and lower detectivity. This explains the absence of the Raman lines on top of the luminescence, as in Fig. 4. As can be appreciated, a change from 77 K to room temperature does not shift the maximum of the peak, implying the absence of thermalization among the electrons in the defects. This is in qualitative agreement with the expectations from the density of defects as obtained from EPR that can be understood as coming from a relatively diluted collection of states ($\sim$ one defect every ten cells). Thermalization among color center is, therefore, unlikely. The main conclusion of this observation is that the luminescence line shape can be considered a fairly good representation of the defect density of states in the gap.

In addition, the temperature dependence of the luminescence intensity measured at the maximum of the peak dis-

plays some sort of consistency with the presence of a resonant behavior for the lattice modes. In effect, we show in the inset to Fig. 6(b) the temperature dependence of the luminescence intensity. It is quite clear from the data that there is a crossover in the relaxation of the luminescence at a temperature of ~ 150 K. This temperature corresponds exactly to the phonon energy of the lattice modes that is ~ 100 cm^{-1}. Thence, we conclude that the electrons producing the luminescence are coupled to the lattice modes of $\omega \sim 100$ cm^{-1} through the electron-phonon interaction and that is, at the same time, consistent with a resonant behavior like the one shown in Fig. 5(b). The stretching modes, on the other hand, have no influence in the luminescence intensity at this temperatures since 2900 cm$^{-1} \sim$ 4100 K.

As mentioned earlier, the fact that the resonance enhancement in Fig. 6(a) is weak has a physical origin and can be traced to the relatively small amount of damaged molecules (0.1%) and, in addition, a natural consequence of a wide inhomogeneous broadening. The former implies that only $\sim 10^{-3}$ of the Raman-scattering processes relative to the studied phonons should be resonantly enhanced, the electronic transitions in the nonirradiated molecules being several eV above the excitation energy. The latter, on the other hand, means that for the scattering occurring *in* damaged molecules in the crystal, there is a strong resonant enhancement only for a narrow collection of states in the gap that coincide in energy with the incident or scattered photons. The Raman signal in this situation is the result of a huge nonresonant contribution provided by all the states in the gap that are not resonant (nondamaged molecules plus irradiated ones with the defect level far away from the incident or scattered photon) plus the resonant contribution of a very small fraction of states that are degenerate with any of the two photons. The ratio of the two can be as small as 10^{-5} and a change by 50% in the *total* intensity produced by these resonant states is equivalent to a resonance enhancement of the order of 10^5, which is typical, in fact, of *strong* Raman resonances. Note also that the spectra used for Fig. 6(a), taken with the nine Ar^+-laser lines, lay in all cases within the luminescence, and thus the scattering is never completely detuned from resonance (the spectrum taken with the He-Ne laser is not included in the figure).

In the next section, we shall discuss a calculation of a simple model defect in irradiated L-alanine that can explain qualitatively these findings.

V. CALCULATION OF THE ELECTRONIC DEFECT

The experimental evidence on the nature of the electronic defect produced by electron irradiation on single crystals of L-alanine can be summarized as follows: (i) the EPR results are consistent with a dangling electron localized at the methyl and CH groups. A simplified model for this unpaired electron that explains the hyperfine coupling constants observed in EPR has been developed by Miyagawa and Itoh.[4](ii) The color centers induced in the gap by irradiation show a density of states, as deduced from the luminescence, with a fairly large inhomogeneous broadening, suggesting a myriad of possible configurations for the ammonium group with respect to the rest of the molecule. (iii) The luminescence of the defects shows a resonant behavior with two types of modes, one at 2900 cm^{-1}, associated with the hydrogen stretching of the methyl group, and the lattice modes around ~ 100 cm^{-1} related to the hydrogen bridges between the ammonium group and the oxygens of the neighbor molecule in the unit cell. (iv) The temperature dependence of the intensity of the luminescence [inset to Fig. 6(b)] evidences the interaction of the electrons in the color centers with phonons of ~ 100 cm^{-1}, which coincide with the energy of the lattice modes. Point (ii) is perfectly consistent with the results of EPR, while points (iii) and (iv) imply also a defect wave function with certain overlap on the ammonium group.

In line with the previous theoretical treatment of the defect by Miyagawa and Itoh we need to reconcile the resonant Raman behavior of the lattice modes as well as the distribution of possible energies for the luminescence emission in the gap with the EPR results. To this end, we need to model the electronic defect including, at the same time, the proximity of the ammonium group that was separated from the molecule by the effect of irradiation. The model defect is constructed by considering an isolated alanine molecule without the ammonium group in the proximity of a NH_3 group that models the breakup of the central C-N bond upon irradiation. The main problem in shaping a proper model for a defect of this type by means of an isolated molecule is to appropriately take into account the effect of the *rest* of the crystal in the charge balance of the molecule, i.e., to suitably consider boundary conditions for the orbitals to model the real situation inside the crystal. This is not an easy task but can be reasonably well overcome to obtain qualitative results.

We assume a model defect with the following characteristics: the C-N central bond of a single alanine molecule is cut and the free nitrogen bond is saturated with an additional hydrogen. This reduces the electron affinity of the ammonium group and simulates the partial compensation produced in the real crystal by the oxygens of the neighbor molecule through hydrogen bonding. At the same time, the oxygens of the COOH group could be saturated with an additional hydrogen to avoid one double bond to the carbon and simulate once more the hydrogen bonding to the neighbor molecule. This has, however, little effect on the ground-state wave function and we therefore leave this group as COOH. In this manner, a dangling bond coming from the unpaired electron in the central carbon of the molecule (CH) is generated on the side of the molecule that is attached to the methyl group. This dangling bond is the electronic state modeled by Miyagawa and Itoh[4] with a simplified version of the orbital wave function involving the methyl group solely. The part of the molecule that contains the methyl group is not allowed to relax its geometry in the calculation after the ammonium group has been separated. This is done because structural relaxation should be to a great extent hindered in the real crystal by the presence of the neighboring molecules. Thence, the self-consistent electronic field of the molecule is calculated for a frozen geometry. The ground-state electronic wave functions are calculated by means of the Austin Model 1 Hamiltonian (AM1) (Ref. 16) and the program MOPAC version VI developed by Stewart,[17] which allows for a simultaneous determination of the hyperfine coupling constants on the different hydrogens of the molecule. The self-consistent electronic field is obtained in the unrestricted Hartree-Fock

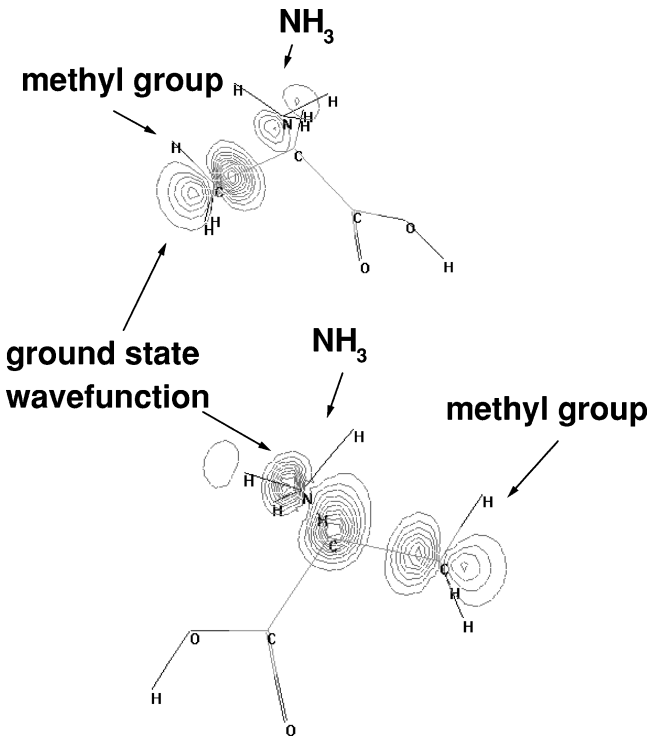

FIG. 7. Two side views of the squared ground-state wave function for the dangling electron in a model defect for irradiated L-alanine. Note the partial overlap of the wave function with the NH_3, CH, and methyl group. This configuration displays absorptions in the visible around $\sim 2.2-2.5$ eV as obtained through a configuration interaction calculation. This type of electronic state can simultaneously explain the existence of luminescence in the visible, resonant Raman scattering with the stretching and lattice modes and the existence of the EPR signal. Further details are given in the text.

mode,[18] which is more reliable for open shell molecules with unpaired electrons and situations describing bond breaking. The squared wave function of the unpaired electron in the ground state is shown in Fig. 7 for a typical separation between the ammonium group and the rest of the molecule. We have picked two views of the wave functions that clearly show that the dangling bond minimizes its interaction with the divided ammonium group by producing a partial overlap of the wave function in the region of the NH_3. We find that such a ground state has the following characteristics: (i) it can interact with phonons that are localized either in the methyl or ammonium groups, (ii) its absorption spectrum obtained through a *configuration interaction*[18] calculation with a proper energy cutoff has peaks in the visible with the largest oscillator strengths in the range $\sim 2.2-2.5$ eV, depending on the exact position of the ammonium group (the gap for the nonirradiated molecules is 7.2 eV) and, (iii) the hyperfine coupling constants in the hydrogens of the methyl group do show an anisotropy of the same order of magnitude as the one deduced in Miyagawa's model[3] and measured experimentally. We obtain for a particular position of the ammonium group the hyperfine constants of 6, 16, and 41 G for the three hydrogens of the methyl group as compared to 5, 27, and 43 G observed experimentally. The hyperfine constant relative to the hydrogen in the CH group is strongly sensitive to the exact position of the ammonium group, and is thus not meaningful within this model.

Notwithstanding the correct qualitative picture, this model defect has to be interpreted as a *demonstration of possibility* for several reasons. First, the saturation of the bonds to model the effect of the rest of the structure is *per se* a simplification but, in addition, the exact position of the ammonium group after the damage has been created is not known, and possible structural relaxations of the damaged molecule can also have an influence on the electronic structure that are not being considered here. Note that the uncertainty in the position of the ammonium group and the possible structural relaxations are, in fact, needed ingredients to explain the huge inhomogeneous broadening observed in the luminescence. This is, at the same time, a source for inhomogeneous broadening for the hyperfine coupling constants since different configurations will have distinct wave functions and, accordingly, different couplings of the spin density to the hydrogens. As a matter of fact, we believe that the observed linewidths in EPR are consistent with the inhomogeneous broadening of the luminescence. The calculation shows qualitatively that it is, in principle, possible to have a ground-state wave function that explains simultaneously the EPR, luminescence, and resonant Raman signals.

VI. CONCLUSIONS

We have shown that resonant Raman scattering and photoluminescence provide additional useful information on the characteristics of the electronic defects created by irradiation in L-alanine. In particular, the wide diversity of modes that these molecules possess allows for multiple possibilities to use these vibrations as local probes for the presence of localized electrons in different parts of the molecules. Resonant Raman scattering complements, in this way, the results obtained by EPR and extends our knowledge on the nature of the defects. We have shown that the wave function of the electronic defect in irradiated L-alanine needs to have some overlap with both the ammonium and methyl groups in order to explain the temperature dependence of the luminescence and the resonant Raman signals.

ACKNOWLEDGMENTS

Special thanks are due to F. Tutzauer, R. Gludovats, C. Eggenschwiler, R. Soto, and B. Eckardt, for the construction and design of different parts of our experimental setup, and to M. Schneebelli and D. D'Avanzo for the irradiation of the samples. Willy Pregliasco is also greatly acknowledged for his participation in the initial stage of these investigations, and for a critical reading of the manuscript. E.W. thanks the Consejo Nacional de Investigaciones Científica y Técnicas for partial financial support.

[1] V. Volkenstein, *Molecular Biophysics* (Academic Press, New York, 1977).
[2] B. Ciesielski and L. Wielopolski, Radiat. Res. **140**, 105 (1994), and references therein.
[3] I. Miyagawa and W. Gordy, J. Chem. Phys. **32**, 255 (1960).
[4] I. Miyagawa and K. Itoh, J. Chem. Phys. **36**, 2157 (1962).
[5] K. Itoh and I. Miyagawa, J. Mol. Struct. **190**, 85 (1988).
[6] H. Muto, M. Iwasaki, and K. Ohkuma, J. Magn. Reson. **25**, 327 (1977).
[7] R. Angelone, C. Forte, and C. Pinzino, J. Magn. Reson. Ser. A **101**, 16 (1993).
[8] K. Machida, A. Kagayama, Y. Saito, and T. Uno, Spectrochim. Acta A **34**, 909 (1978).
[9] D. M. Byler and H. Susi, Spectrochim. Acta A **35**, 1365 (1979).
[10] J. Bandekar, L. Genzel, F. Kremer, and L. Santo, Spectrochim. Acta A **39**, 357 (1983).
[11] M. Cardona, in *Light Scattering in Solids*, edited by M. Cardona and G. Güntherodt (Springer, Berlin, 1982), Vol. 2.
[12] M. S. Lehmann, T. F. Koetzle, and W. C. Hamilton, J. Am. Chem. Soc. **94**, 2657 (1972).
[13] These values are assessed by a simple calculation of the normal modes using the AM1 Hamiltonian. These modes will be modified in reality due to either solvent effects, in the case of the isolated molecule, or neighbor interactions, in the case of the crystal.
[14] C. H. Wang and R. D. Storms, J. Chem. Phys. **55**, 5110 (1971).
[15] A. Migliori, P. M. Maxton, A. M. Clogston, E. Zirngiebl, and M. Lowe, Phys. Rev. B **38**, 13 464 (1988).
[16] W. Thiel, Tetrahedron **44**, 7393 (1988).
[17] J. J. P. Stewart, in *Reviews in Computational Chemistry*, edited by K. B. Lipkowitz and D. B. Boyd (VCH, New York, 1990), Vol. 1, p. 45.
[18] M. J. S. Dewar, *The Molecular Orbital Theory of Organic Chemistry* (McGraw-Hill, New York, 1969); W. J. Hehre, L. Radom, P. v. R. Schleyer, and J. A. Pople, *Ab Initio Molecular Orbital Theory* (Wiley, New York, 1986).